JOURNAL OF SPACECRAFT AND ROCKETS
Vol. 36, No. 1, January–February 1999

Flight Data for Boundary-Layer Transition at Hypersonic and Supersonic Speeds

Steven P. Schneider
Purdue University, West Lafayette, Indiana 47907-1282

Published flight data for boundary-layer transition at hypersonic speeds are surveyed. The survey is limited to measurements reported in the open literature and carried out at hypersonic and high-supersonic speeds, on vehicles for which ablation is believed to be negligible or small. The emphasis is on work that may be suitable for validation of advanced transition-estimation methods that are based on simulation of the physical mechanisms, such as e^N, the parabolized stability equations, and direct numerical simulations. Brief discussions are presented for each report. Known comparisons to the advanced simulation methods are also presented.

Nomenclature

M_e = Mach number at the boundary-layer edge
Re_s = Reynolds number at transition onset, based on arc length from the leading edge and local conditions at the boundary-layer edge
Re_T = Reynolds number at transition onset, based on arc length and conditions at the boundary-layer edge
Re_T/ft = unit Reynolds number per foot, at the boundary-layer edge at transition onset
Re_θ = Reynolds number at transition, usually onset, based on momentum thickness and conditions at the boundary-layer edge
T_e = temperature at the boundary-layer edge
T_r = recovery temperature at the wall
T_w = wall temperature
x_T = arc length to transition onset, from the nose
θ_c = cone half-angle, deg

Introduction

LAMINAR–TURBULENT transition in high-speed boundary layers is important for prediction and control of heat transfer, skin friction, and other boundary-layer properties. However, the mechanisms leading to transition are still poorly understood, even in low-noise environments.[1] Applications hindered by this lack of understanding include reusable launch vehicles, such as the X-33, high-speed interceptor missiles,[2,3] hypersonic cruise vehicles,[4] and re-entry vehicles.[5] Transition in high-speed shear layers is also important for accurate prediction of shock–shock interactions.[6]

The transition process is initiated through the growth and development of disturbances originating on the body or in the freestream.[7] The receptivity mechanisms by which the disturbances enter a boundary layer are influenced by roughness, waviness, bluntness, curvature, Mach number, and so on. The growth of the disturbances is determined by the instabilities of the boundary layer. These instabilities are in turn affected by all of the factors determining the mean boundary-layer flow, including Mach number, transverse and streamwise curvature, pressure gradient, and temperature.[1] Relevant instabilities include the concave-wall Görtler instability,[8,9] the first and second mode Tollmien–Schlichting (TS)-like instability waves described by Mack,[10] and the three-dimensional crossflow instability.[11] The first appearance of turbulence is associated with the breakdown of the instability waves, which is determined by various secondary instabilities.[12] Local spots of turbulence grow downstream through an intermittently turbulent region, whose length is dependent on the local flow conditions and on the rate at which spots are generated.[13]

In view of the dozens of parameters influencing transition, classical attempts to correlate the general transition point with one or two parameters, such as Reynolds number and Mach number, can only work for cases that are similar to those previously tested. Transition-estimation methods that are reliable for a broad range of conditions will need to be based on an understanding of the physical mechanisms involved. Improvements in techniques for estimating the location and extent of transition will depend on improvements in our understanding of the physical mechanisms involved.

The simplest and best developed of the mechanism-based methods are the e^N methods, which attempt to correlate transition with the integrated growth of the linear instability waves. Although these methods neglect receptivity and all nonlinear effects, such as wave interactions, nonlinear breakdown effects, roughness, and so on, they have shown promising agreement with experiment.[1] Agreement is fairly good for a variety of conditions where the environmental noise is generally low.[14] However, the accuracy of many high-speed e^N computations remains uncertain, for it is often not clear whether bluntness effects, wall temperature distributions, and so on were handled with sufficient accuracy.[15] Although wave interaction effects and three-dimensional effects can sometimes be handled with correlations,[16] e^N methods are only an intermediate step along the way to reliable mechanism-based methods.

Direct simulations of transition[17] and the recently developed parabolized stability equations (PSE)[18,19] have in some ways advanced theoretical–numerical work far ahead of the experimental database. The numerical work is not yet able to include complex

Steven P. Schneider is an associate professor in the School of Aeronautics and Astronautics at Purdue University. He received his B.S. (engineering and applied science), M.S. (aeronautics), and Ph.D. (aeronautics, 1989) from the California Institute of Technology. Dr. Schneider has been conducting experimental research in boundary-layer transition since 1986. Since 1989, his work has focused on high-speed transition, the development of quiet wind tunnels, and measurements of the mechanisms of transition. He is a Senior Member of the AIAA.

Received Oct. 31, 1997; revision received Oct. 1, 1998; accepted for publication Nov. 13, 1998.

effects such as roughness, waviness, internal shocks, and most bypasses. Three-dimensional mean flows and their instabilities are only beginning to be treated correctly from first principles.[20] The simulation of bluntness effects[21] and chemistry effects[22,23] from first principles is only beginning. When the numerics are based on the correct physical mechanisms, however, they can provide much more detail regarding the transition process. Experimental work that describes not only the location of transition but also the mechanisms involved is needed to improve these modern theories. The key mechanisms need to be identified, in part through experimental work, and the key numerical results need to be validated experimentally.

Unfortunately, most of the ground-test data are ambiguous, due to operation in high-noise conventional wind tunnels and shock tunnels, with disturbance levels much higher than in flight.[24] The mechanisms of transition operational in small-disturbance environments can be changed or bypassed altogether in high-noise environments.[25] Pate and Schueler[26] showed that transition measurements in conventional tunnels can be correlated by tunnel-wall boundary-layer noise parameters alone, independent of Mach number. Pate[27] concludes that "if a true Mach number effect exists, it is doubtful it can be determined from data obtained in conventional supersonic/hypersonic wind tunnels because of the adverse effects of facility noise." Just as at low speed, ground tests must be conducted at noise levels comparable to flight to provide reliable and unambiguous measurements of transition mechanisms and trends.

Flight tests are free from facility noise issues and must constitute the final basis for evaluating transition-estimation techniques. Flight tests have their own limitations.

1) There is limited characterization of atmospheric conditions and flight conditions.

2) There is limited instrumentation. Measurements are nearly always restricted to temperature sensors placed at or below the surface, with the possible addition of a few pressure measurements. Transition location is usually inferred from heat transfer data, but there is usually no data on the instability mechanisms that caused the transition.

3) The test body is usually not retrieved, and tests are rarely repeated, so that conditions are sometimes ambiguous.

4) The roughness of the test body during flight is unknowable if the body is not recovered; roughness before flight is rarely characterized with sufficient care. Steps, gaps, and waviness during flight are rarely knowable. Small roughness defects sometimes create unusual transition patterns in ground tests and are so identified and removed; such iterative finish checks are not available in flight test.

5) The test vehicle can deform in flight due to heating loads; these deformations are rarely characterized with great care.

6) The wall temperature distribution is rarely known in great detail and is probably always nonuniform.

7) For hypersonic tests, even those designed to have minimal ablation, some ablation is still expected on the nosetip. The amount of ablation is usually not measured.

8) Angle of attack is difficult to control in flight, and angles of 1 deg can affect transition substantially if the included angle of the body is small. Angle of attack is rarely measured with sufficient care; in most tests, it is not measured at all.

In addition, flight tests are very expensive. The cost of the ride to Mach 12 has been quoted as $50 million to $60 million, not including the test article, instrumentation, and data reduction.

A large number of high-speed flight tests have been carried out over the past 50 years, most of them to study the problem of ballistic re-entry. The current interest is primarily in reusable nonablating vehicles, and a number of flight tests with zero or minimal ablation exist, although they are scattered through a large literature. Because many of the workers familiar with this literature are retiring, and because almost none of the community is familiar with the full span of this work, this survey was written to catalog it in one accessible place. This survey, updated from Ref. 28, almost certainly remains incomplete; the author would appreciate having additional work brought to his attention.

Many of these expensive tests appear to be documented well enough to allow accurate and detailed modern computations of the mean flow, enabling estimations of transition location using e^N, PSE, or direct numerical simulation methods, for comparison to the measurements. The original mean flow computations are in many cases very limited, due to the limited computational fluid dynamics capabilities available to the authors. In many cases even the mean flow properties, such as the boundary-layer thicknesses, have not been computed with reasonable accuracy, if at all. It appears that the boundary-layer transition community may have much to gain from reanalyzing these expensive tests and comparing the results to predictions from modern analysis techniques.

A detailed analysis of the flight database will require extensive resources because computations of various flight conditions need to be carried out with good accuracy just to determine whether the mean flow can be computed with reasonable agreement. For example, computations will have to be carried out at zero and small angles of attack, for many flight conditions, to determine if the thermocouple data in many reports are consistent with the nominally zero angle of attack often claimed. This author does not currently have the resources to carry out these extensive computations, and it appears that there is little prospect that any single group will be able to carry out a major program of this type in the near future. However, if the community was more generally aware of the quantity and quality of available flight data, perhaps resources might be found to carry out some of these simulations on a piecemeal basis.

The computational predictions presented here are almost never accurate and reliable enough to be final and conclusive. Similarly, the flight data suffer from the limitations described earlier, and it remains to be determined whether any of it is sufficiently well documented and consistent to allow its use as a conclusive benchmark for code validation. The intent of this survey is, therefore, to facilitate access to the flight database and to begin the process of identifying those tests that may be suitable for detailed comparison to modern simulations.

Comment on Ballistic-Range Data

Only free-flight data will be surveyed because the ballistic-range data (which are also called free-flight data) may warrant a separate review. The cause of the relatively low transition Reynolds numbers observed there remains controversial, as is the cause of the unit Reynolds number effect observed on nominally sharp cones at nominally zero angle of attack. The range data suffer from many of the difficulties of the flight data because the models are usually not recoverable. Malik et al.[29] have suggested via e^N studies that the very small bluntness (0.005 in.) specified for Potter's models is sufficient to explain the unit Reynolds number effect in Potter's range data, e.g., see Ref. 30. The same nose bluntness was specified for Reda's[31] work, which exhibits a similar unit-Reynolds number effect. Reda explains the specification as follows: "A model nosetip radius of 0.005 in. was selected to ensure complete entropy swallowing within the initial 1.0 in. of wetted length measured from the stagnation point; measured run lengths to transition were greater than 2.5 in. and thus all data were obtained in the sharp-cone regime." Although it is not clear from the Malik et al. report whether their computations corroborate Reda's swallowing-length estimates, it appears that the 0.005-in. specification is inadequate. Even if transition occurs downstream of the swallowing zone, the bluntness will still affect the growth of the waves within the swallowing region and, thus, the integrated growth of the waves at all positions downstream. Because the computations of Malik et al. were carried out at Mach 8 and do not duplicate the conditions of Potter's work at Mach 5, the issue remains to be resolved conclusively.

Previous Surveys

Several previous surveys of this literature have appeared, usually with a focus on algebraic correlations of transition location.

Beckwith and Stainback, Circa 1975

Reference 32 contains a plot of flight and ground-test data for transition "on sharp cones in wind tunnels and flight" (Fig. 4, Ref. 32). The Ref. 32 figure has been reproduced several times in various general reviews, for example, by Stetson (Fig. 17, Ref. 33). Although Ref. 32 cites Ref. 34 for detailed information regarding the data presented in the figure, detailed references are not actually presented there. The symbols used in the figure are nowhere defined.

Table 1 Flight data tabulated in Tables 2 and 3; most plotted in Fig. 4 of Ref. 32

IEB no.	Reference	No. points used	Present ref. no.
12	Rabb and Disher, NACA RM-E55I15	7	36
13	Rabb and Simpkinson, NACA RM-E55F27	5	37
14	Merlet and Rumsey, NASA TN-D-951	8	38
15	Rumsey and Lee, NASA TN-D-824	4	39
16	Rumsey and Lee, NASA TN-D-745	4	40
17	Rumsey and Lee, NASA TN-D-888	20	41
21	Krasnican and Rabb, NASA MEMO 3-4-59F	4	42
22	Disher and Rabb, NACA RM-E56G23	4	43
34	Chauvin and Speegle, NACA RM-L57D04	3	44
54	Re-Entry F, Wright and Zoby, AIAA Paper 77-719	7	45
58	Sherman and Nakamura, AIAA Paper 68-1152	4	46
Total number of points		70	

Most of the flight data shown in the figure were also presented (and referenced) in Ref. 35; however, this reference also refers to classified re-entry flights, and even after 30 years, distribution is still restricted to U.S. nationals. Although a NASA technical memorandum describing the survey is cited as being in preparation in Ref. 35, the survey was never published, according to P. C. Stainback and I. E. Beckwith (IEB) in a private communication in 1997.

The references (herein Refs. 36–46) for Fig. 4 in Ref. 32 were supplied by Stainback and Beckwith, from unpublished notes; they are published here, in Table 1, for the first time. The tabulated data are the result of a search for flight data for sharp cones at zero angle of attack. The user should be aware that not all of the cones were really sharp and that the angle of attack is in many cases not really zero.

The IEB number is the reference number from Beckwith's and Stainback's notes. There are a total of 77 flight data points plotted in IEB's Fig. 4 (Ref. 32), and IEB Refs. 21, 22, and 34 were not used in making the plot, so that 18 of them are not accounted for. Stainback and Beckwith believe that the other 18 points probably came from classified sources, such as those mentioned in Ref. 35. Copies of the tables used to plot the Ref. 32 Fig. 4 were provided by Stainback. Key parameters from the flight data are given here in Tables 2 and 3; these values were transcribed directly from Stainback and Beckwith's notes, and although Tables 2 and 3 were proofed by Stainback against his notes, they have not been further checked. Dashes are shown in cases where Beckwith and Stainback do not provide a value. In several places two edge temperatures are shown, and the cause is not known; one may be drawn from a sharp-nose analysis and the other from a blunt-nose analysis. For IEB's Ref. 16, nine values are shown in Table 2, yet only four are listed as being in IEB's plot. The other five points are flagged (in Ref. 40) to show transition did not occur at the sensor, and these points were not included. The first two points listed in Table 2 for IEB's Ref. 14 are also "transitional," meaning that the value of the Nusselt number lay between the theoretical values for laminar and turbulent flow; however, they were included in the plot anyway. The blunt-nose data in IEB Ref. 22 (herein Ref. 43) are presented twice: the footnoted blunt and sharp rows given in Table 3 are different analyses of the same flight data using blunt- and sharp-nose assumptions for computations of the local conditions. There are additional data in IEB's Ref. 22, but these were not included in the tabulation, for unknown reasons. Also, some of the values for x_T given in IEB's Ref. 22 are apparently in error to some extent because the unit Reynolds numbers and the x_T values do not agree with the Reynolds number Re_T values.

In addition to the values shown in Tables 2 and 3, other values are shown in Beckwith's and Stainback's unpublished table, the specific ones depending on the citation.

The data from Tables 2 and 3 are plotted in Fig. 1. IEB's Fig. 4 does not plot the data here labeled as blunt (IEB Refs. 21, 22, and 34). Although the remainder of the data plotted in Fig. 1 are nominally limited to data from sharp cones, the bluntness in some of the flights may not be negligible (see Ref. 35 for the criterion apparently used). Most of the high Mach number data plotted by IEB came from the re-entry F experiment, as can be seen by comparing the present Fig. 1 with IEB's Fig. 4. IEB plots an additional

Table 2 Flight data tabulated by Beckwith and Stainback, part 1 of 2

IEB no.	θ_c	T_w/T_e	M_e	$Re_T \times 10^{-6}$	$Re_T/\text{ft} \times 10^{-6}$	x_T, ft	T_e, °R
12	10	1.27	3.9	17.4	17.9	0.97	520
12	10	1.25	3.8	19.9	16.85	1.18	513
12	10	1.31	3.7	24.4	16.01	1.522	509
12	10	1.22	3.65	26.6	15.2	1.748	507
12	10	1.18	3.6	29.0	14.8	1.96	501
12	10	1.20	3.6	31.9	14.8	2.155	501
12	10	1.27	3.4	27.7	14.1	1.96	499
13	10	——	2.25	8	6.32	1.266	452
13	10	——	2.30	8.2	6.43	1.275	452
13	10	——	2.20	8.75	6.09	1.437	450
13	10	——	1.70	7.85	4.46	1.757	430
13	10	——	1.70	8.50	4.46	1.908	430
14	5	——	3.28	22.1	22.1	1.0	550
14	5	——	3.48	22.4	22.4	1.0	547/523
14	5	——	3.31	28.8	20.2	1.415	536
14	5	——	3.15	33.1	18.1	1.832	527/504
14	5	——	3.01	23.0	16.3	1.415	521
14	5	——	2.78	19.1	13.5	1.415	508
14	5	——	2.17	10.8	7.6	1.415	462/444
14	5	——	1.96	6.1	6.1	1.0	440
15	7.5	——	2.85	3.8	7.0	0.541	430/427
15	7.5	——	3.66	4.6	8.5	0.541	448
15	7.5	——	4.12	6.1	9.1	0.667	458
15	7.5	——	4.25	8.0	8.7	0.916	459
16	5	1.18	1.57	9.2	7.9	1.166	507
16	5	1.18	1.87	10.9	9.4	1.166	509
16	5	1.23	2.56	14.8	12.7	1.166	512
16	5	1.24	2.92	16.9	14.5	1.166	516
16	5	1.27	3.38	19.4	16.7	1.166	514
16	5	1.80	3.76	13.6	16.3	0.833	532
16	5	1.95	3.72	12.9	15.5	0.833	493
16	5	2.18	3.65	10.9	13.1	0.833	446
16	5	2.30	3.62	10.0	12.2	0.833	424

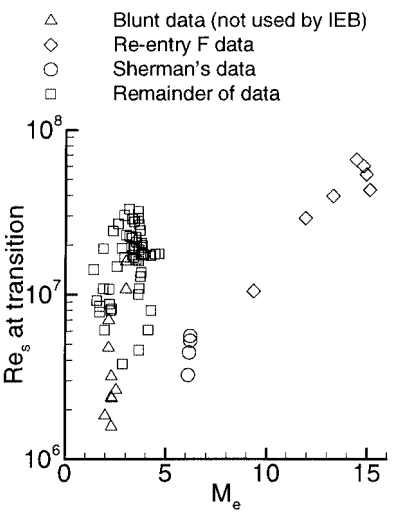

Fig. 1 Correlation of transition Reynolds number data on sharp cones in wind tunnels and in flight (adapted from Beckwith[32]).

18 points between $M_e \simeq 7$ and $M_e \simeq 12$; the sources for these data apparently remain classified. Apart from re-entry F, the blunt data, the Sherman and Nakamura (IEB Ref. 58) data, and IEB Ref. 15, most of the data lie in a cluster between $M_e \simeq 1.5$ and $M_e \simeq 5$ and between $Re_s = \simeq 6 \times 10^6$ and $Re_s \simeq 35 \times 10^6$. The wall temperature and roughness vary considerably, along with angle of attack, so that detailed consideration of the flight conditions will be necessary for development of reliable transition-estimation techniques. Brief summaries of these conditions are contained in the following sections.

Martellucci et al.,[47] 1972, and Berkowitz et al.,[48] 1977

Reference 47 cites and analyzes a large database of flight data for transition on re-entry vehicles. Reference 48 is a later and more accessible version, which contains similar information. Martellucci

Table 3 Flight data tabulated by Beckwith and Stainback, part 2 of 2

IEB no.	θ_c	T_w/T_e	M_e	$Re_T \times 10^{-6}$	Re_T/ft $\times 10^{-6}$	x_T, ft	T_e, °R
17	7.5	——	1.41	14.2	6.8	2.08	508
17	7.5	——	1.87	19.0	9.1	2.08	509
17	7.5	——	2.36	24.3	11.7	2.08	517
17	7.5	——	2.61	26.9	12.9	2.08	522
17	7.5	——	2.91	30.3	14.6	2.08	530
17	7.5	——	3.17	22.6	15.9	1.915	530
17	7.5	——	3.49	16.4	17.9	0.916	538
17	7.5	——	3.74	17.5	19.1	0.916	535
17	7.5	——	3.84	17.7	19.3	0.916	538
17	7.5	——	3.81	19.3	18.6	1.042	531
17	7.5	——	3.75	20.6	17.6	1.166	525
17	7.5	——	3.63	18.7	16.0	1.166	516
17	7.5	——	3.52	20.8	14.7	1.416	506
17	7.5	——	3.42	19.0	13.4	1.416	497
17	7.5	——	3.33	17.4	12.2	1.416	485
17	7.5	——	3.37	16.8	11.8	1.416	480
17	7.5	——	3.61	16.0	12.4	1.291	479
17	7.5	——	4.23	17.2	13.3	1.291	468
17	7.5	——	4.45	17.6	13.6	1.291	463
17	7.5	——	4.64	17.7	13.7	1.291	459
21	7.5	blunt	2.30	0.77	2.91	0.264	746
21	7.5	blunt	2.30	1.58	2.92	0.541	746
21	7.5	blunt	2.30	2.38	2.91	0.818	746
21	7.5	blunt	2.30	3.19	2.91	1.095	746
22	7.5	blunt[a]	2.15	4.75	5.85	0.812	697
22	7.5	blunt[a]	2.15	7.0	5.82	1.202	697
22	7.5	sharp[a]	3.00	10.75	12.7	0.846	479
22	7.5	sharp[a]	3.00	15.9	12.7	1.252	479
34	25	——	1.99	1.84	22.1	0.083	691
34	25	——	2.32	2.34	28.1	0.083	768
34	25	——	2.53	2.63	31.6	0.083	836
54	5	——	15.10	43.0	4.507	——	——
54	5	——	14.93	53.5	7.110	——	——
54	5	——	14.78	60.0	8.43	——	——
54	5	——	14.43	65.6	10.05	——	——
54	5	——	13.29	39.5	8.585	——	——
54	5	——	11.93	29.0	7.45	——	——
54	5	——	9.34	10.5	3.912	——	——
58	22	$T_w/T_r = 0.09$	6.20	5.6	——	——	——
58	22	$T_w/T_r = 0.10$	6.20	5.25	——	——	——
58	22	$T_w/T_r = 0.12$	6.15	4.45	——	——	——
58	22	$T_w/T_r = 0.12$	6.10	3.25	——	——	——

[a]Different analyses of same data using blunt- and sharp-nose assumptions.

et al.[47] and Berkowitz et al.[48] considered approximately 200 vehicles and selected 40 of these, based on data quality, small angle of attack, and the use of simple sphere-cone geometries. A uniform set of detailed flowfield computations were then performed for each vehicle. These papers[47,48] are valuable surveys of the (mostly classified) re-entry literature but are primarily focused on algebraic correlation techniques for estimating transition. Unfortunately, much of the primary re-entry literature is still classified or limited, and so information sufficient to allow detailed computations is rarely available.

Figures 15 and 16 from Ref. 47 show flight data plotted in Reynolds numbers Re_s and Re_θ vs Mach number M_e coordinates; the data from the nonablating frustra in the Ref. 47 figures are replotted here as Fig. 2. Data are plotted for four different combinations of the materials used for the nosetip and frustrum. For each of these four combinations, the transition-onset value of Reynolds number Re_s is shown with open symbols, and the transition-onset value of Reynolds number Re_θ with filled symbols. Three of the combinations have beryllium frustra (BE), and one has an Inconel frustrum. The nosetip materials are graphite (ATJ, 11 pts.), phenolic-graphite (PG, 2 pts.), silica-phenolic (SP, 4 pts.), and SS (1 pt.), which is apparently stainless steel, although it is not defined in Ref. 47. The effect of ablation on the nosetips is probably not negligible.

The Reynolds number Re_θ vs Mach number M_e coordinates plotted are often used in first-order correlations. Note that even for this restricted subset of the data, Reynolds number Re_θ scatters about a factor of about 3 at a given Mach number M_e. Because this scatter causes Reynolds number Re_s to scatter by a factor of about 9, the value of such correlations is limited.

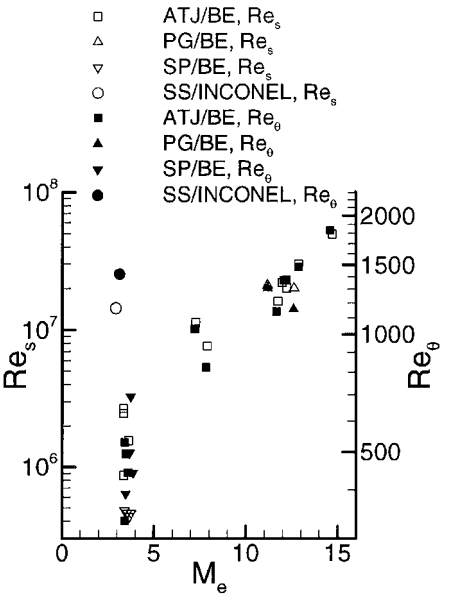

Fig. 2 Flight data correlation using frustrum parameters (adapted from Martelluci et al.[47]).

Batt and Legner,[49,50] 1981 and 1983

References 49 and 50 contain a comprehensive survey of transition on hemispherical nosetips under re-entry conditions. Although the focus of the survey is on transition on ablating nosetips with rough surfaces, some data for nonablating nosetips are also presented (Sec. C in Ref. 50). A correlation is presented for roughness-induced transition on the subsonic portion of hemispherical noses. Table 2 in Ref. 50 shows computations for four flights (discussed subsequently) for which Reynolds number Re_θ varies from 300 to 1200 at transition. Batt and Legner emphasize that they looked only at cases where transition occurred on the subsonic portion of the nosetip. The data for transition on ablating nosetips are also reviewed in Ref. 51. Because both of these valuable reviews are mainly concerned with transition on ablating nosetips, their overlap with the present scope is limited.

Williamson,[52] 1992, and Iliff and Shafer,[53] 1993

Reference 52 reviews general flight-test issues. Figure 27 of Ref. 52 is of interest because it shows Reynolds number Re_θ vs Mach number M_e for three-dimensional transition data obtained on the SWERVE vehicle (as discussed in Ref. 53). Figure 27 of Ref. 52 is reproduced here as Fig. 3. Here, M_e is the edge Mach number at the location of transition. Scatter is a factor of 3 or more. The following is from a private communication from Kuntz and Williamson at Sandia.

> The transition data presented in this figure are based on the SWERVE III flight test in which a single maneuvering reentry vehicle executed a high-altitude pull-out, followed by several maneuvers. These maneuvers resulted in the boundary layer at various locations on the vehicle repeatedly transitioning from laminar to turbulent and back again. The local state of the boundary layer was determined both with near-surface thermocouples mounted in plugs within the silica-phenolic heatshield and with photodiode transition measurement devices. The boundary layer edge conditions presented in the figure were calculated with inviscid/boundary layer codes developed at Sandia National Laboratories. The NASP criterion presented on the figure is the relation $Re_\theta = 150 M_e$ which was proposed early in the NASP program as a "generic" transition criterion for maneuvering hypersonic vehicles.

Ablation may not be negligible. According to both Iliff and Williamson (private communications, September 1996), these two papers[52,53] contain all of the available open-literature information on the SWERVE results. Reference 53 also contains details on the X-15, re-entry F, and Shuttle tests, some of which relate to transition.

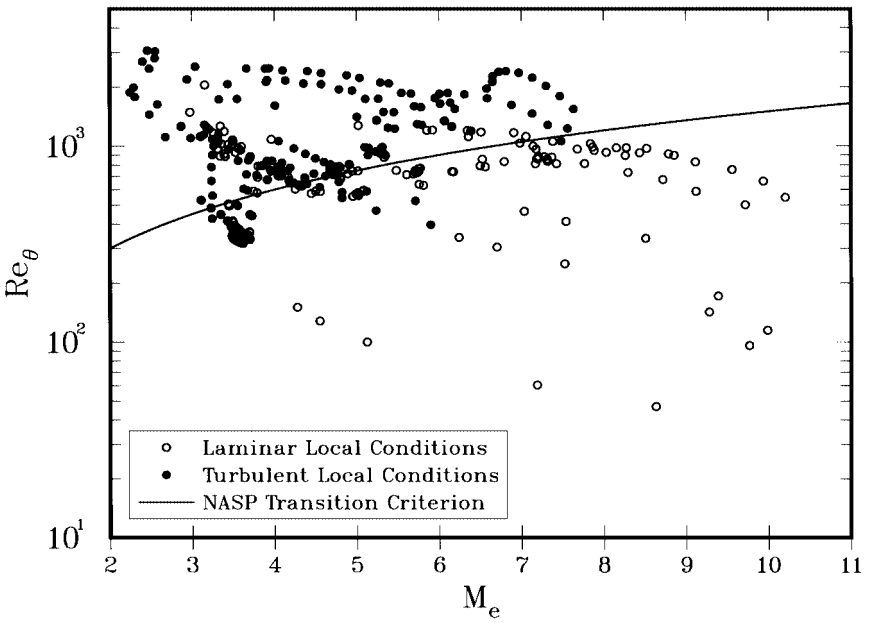

Fig. 3 Comparison of laminar and turbulent flow conditions compared to National Aerospace Plane transition criterion (from Williamson[52]).

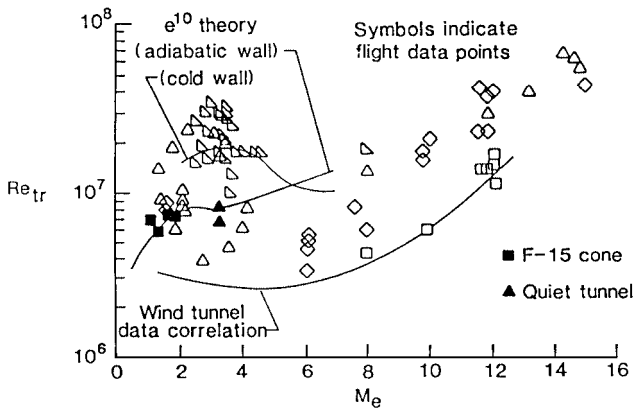

Fig. 4 Comparison of predicted and observed transition Reynolds numbers on sharp cones (from Malik[14]).

Malik[54] e^N Review, 1984

Reference 54 reviews e^N techniques, and compares e^N predictions to quiet-tunnel data and to Fisher and Dougherty[55] and Dougherty and Fisher[56] flight tests at Mach 1.2–1.92. Considerable detail about the e^N computations is reported. The N factors at transition were 8–11.

Malik[14] e^N Review, 1989

Reference 14 discusses the e^N method for hypersonic and supersonic flows. Results are presented for flat plates and round cones at zero angle of attack and are compared to wind-tunnel data. Comparisons to Beckwith's[32] collection of flight data are also presented, by plotting $N = 10$ transition predictions for sharp round cones with 5-deg half-angles, with adiabatic and cold walls. Figure 4 shows the results. At low Mach numbers, the first-mode instability dominates, and the cold walls that are often present act to delay transition. At higher edge Mach numbers, the second mode is dominant, and cold walls move transition upstream. The computations shown in Fig. 4 are only schematic because they were carried out for an arbitrary generic wall temperature. Predictions using e^N are also made for flat plates and round cones at various Mach numbers and temperature conditions, showing scatter of a factor of 3 compared to the Reynolds number/Mach number (Re_θ/M_e) correlation.

High-Enthalpy Hypersonic Tests

This section surveys flight tests carried out on re-entry vehicles at relatively high enthalpy.

X-17 Re-entry

The X-17 program involved a number of re-entry flights, most of which are still classified or limited. Data are reported in the open literature for two polished hemispherical-nose bodies.[57,58] The velocity and altitude during re-entry are given, although the atmospheric conditions are not. The vehicles were rocket powered during the high-energy stage of re-entry to increase the Mach number. The peak velocity was about 13 kft/s at an altitude of 40 kft, and the nose diameter was 9 in. Dissociation effects were significant (Ref. 58, p. D-3). The R-2 vehicle had a copper nose that was polished to a 2-μin. finish, as described in great detail in Ref. 58. The angle of attack during the re-entry was about 3 deg (Ref. 58, p. 36). The R-9 vehicle had a nickel-plated copper nose that was polished to a 1-μin. finish; a 30-μin. patch was installed over the secondary thermocouple run. Both vehicles had a 5/8-in. wall thickness, were instrumented with 23 thermocouples placed along four rays, and had three pressure gauges. The temperature data were reduced to surface heat transfers using axisymmetric and three-dimensional heat transfer computations. The results are compared to analysis performed with equilibrium real-gas assumptions. Transition is inferred from the rise in surface heat transfer.

For R-2, transition occurred at lower values of Reynolds number Re_θ for locations nearer to the stagnation point. Figure 17 in Ref. 57 shows transition onset at $Re_\theta \simeq 350$ at 30 deg from the stagnation point and $Re_\theta \simeq 800$ at 60 deg. According to Ref. 57 (p. 22), the transition onset location on R-2 creeps forward until it reaches the sonic point (about 40 deg aft of the stagnation point), after which the subsonic region of the boundary layer suddenly becomes transitional. Reference 58 agrees that transition flashed suddenly forwards, but states that this began with transition well aft of the sonic point (Ref. 58, p. 81). Figure 29 in Ref. 58 shows asymmetric transition locations, which may have resulted from the small angle of attack.

The R-9 data suffered from noisy telemetry. Transition on the R-9 vehicle was asymmetric, with earlier transition occurring downstream of the roughness patch. Heat transfer over the roughness patch was about twice the value on the other side, and so Ref. 57 takes circumferential heat transfer in the 5/8-in.-thick wall into account when analyzing the thermocouple data. Wall temperatures are reported, but computations of the boundary-layer edge temperature are not. Stagnation point heating agrees well with the Fay–Riddell theory. The good R-9 data are primarily for laminar-flow conditions; little useful transition data exist. The authors[57] believed that the boundary layer remained intermittent on much of the nose and was never fully turbulent. Reanalysis of transition extent and roughness appears to be possible and warranted.

The measurements showed that transition occurred much before it was expected; late transition was originally expected due to the cold wall and the favorable pressure gradient on the nose. It is sometimes argued that this early transition can be completely explained by roughness (such as the roughness that might have developed on the X-17 during flight). However, most workers believe that roughness cannot explain the effect and have called this unexpected early transition the blunt-body paradox.[59,60]

Mark 2 Re-entry

Some data for these classified re-entry vehicle tests are presented in Ref. 61. The vehicles had copper heat-sink noses, but the information given for the flight conditions is very incomplete.[57] The vehicle was instrumented with 17 thermocouples mounted 0.030 in. below the surface and two more mounted deep in the heat shield. The thermocouple temperatures were reduced to surface heat transfers. The data show the onset but not the end of transition. The measurements shown indicate onset at $Re_\theta \simeq 100$–400, much before it was expected; late transition was originally expected due to the cold wall and the favorable pressure gradient on the nose. Transition occurs at lower values of Reynolds number Re_θ in the nose region, another example of the blunt-body paradox. Figure 19 in Ref. 57 shows that the wall enthalpy divided by the freestream stagnation enthalpy was about 0.3–0.1 for the Mark 2 data (see also Fig. 11 in Ref. 61), with Reynolds number Re_θ at transition increasing from 150 to 500 as the wall enthalpy dropped. The open-literature data appear insufficient to allow recomputation of these flows.

Re-entry F

This flight test is documented in Ref. 45. Re-entry of a 13-ft cone with a half-angle of 5 deg and a initial nose radius of 0.1 in. was studied. Lower and upper bounds for ablation of the graphite nosetip during the flight were estimated. The nosetip radius at 80 kft is between 0.14 and 0.19 in. An 0.040-in. backward-facing step between the nosetip and the beryllium heat shield " . . . prevented a forward-facing step during the data acquisition period" (Ref. 62, p. 4). The surface roughness is otherwise not given in the open literature. Measurements were obtained with 84 thermocouples placed primarily on diametrically opposed rays. Four thermocouples were placed at each of 21 locations, at different depths in the beryllium skin, and 13 pressure sensors were also used. Three methods of data reduction are used to infer transition; the most reliable are based on inferring heating rates from the temperature data.

Transition was observed between altitudes of 100,000 and 60,000 ft, when the freestream Mach number was about 20. Because the total enthalpy ranged from 7900 to 7300 Btu/lb (18.3 to 16.9 MJ/kg), this was a hot hypersonic flow test, with real chemistry effects. The angle of attack was less than 0.75 deg during the prime data acquisition period, although at lower altitudes thermal distortion began to become significant (Ref. 63, p. 5). However, the end of transition is substantially asymmetric, even at the higher altitudes. Reference 63 presents blunt-nose equilibrium-air computations for the boundary layer. Figure 5 in Ref. 63 shows that the entropy-layer swallowing length is roughly halfway down the cone; that is, Mach number M_e reaches a value near the sharp-cone value of about 15 at a position that varies from about 3 to about 7 ft with altitude. The wall temperature was nearly equal to the edge temperature (cold wall) at the higher altitudes, but became hot at the lower altitudes. Figure 7e in Ref. 63 shows the wall enthalpy divided by the edge enthalpy at 80 kft; it drops from 1 near the nose to 0.1 at the end of the nosetip to 0.03 over much of the skin.

Depending on altitude, the onset of transition was observed at values of Reynolds number Re_s based on freestream conditions that ranged from 19 to 22×10^6, whereas Reynolds number Re_s based on the local edge conditions ranged from 44 to 68×10^6. At the end of transition, Reynolds number Re_s based on freestream conditions ranged from 30 to 120×10^6, whereas Reynolds number Re_s based on edge conditions ranged from 107 to 240×10^6 (at 60,000 ft, $x_{T,\text{end}}/x_{T,\text{onset}}$ was a remarkable 5.35). Although there is some uncertainty in the local conditions due to problems involved in estimating the nose radius as a function of time during ablation, the experiment is well documented.[62–64] The boundary-layer conditions presented in the reports should be used with caution, however, because all of the computations were performed with early codes and some completely neglect bluntness. Modern mean-flow computations have been performed,[65,66] but the results have not been reduced to quantities of interest for transition research. Tables I and II in both Refs. 45 and 64 list the boundary-layer thickness, but the units are wrong, and the values are in error. The thicknesses are probably in feet instead of inches and are, therefore, off by a factor of 12 (private communication, Zoby, August 1996). Transition was observed to be farther forward on the windward ray, compared to the leeward ray, contrary to most wind-tunnel investigations (Ref. 45, p. 4). Reference 64 gives detailed trajectory information.

Malik et al.[67] have performed e^N computations for this vehicle, for one point in the flight test. The second mode is dominant, and the frequencies range from 160 to 270 kHz. Nose bluntness effects begin to decay at around 0.7 m from the nose; transition occurred at 2.9 m. The reference shows that the N factor at transition was about 7.5. Malik et al. speculate that the somewhat low N factor may be caused by disturbances generated at the joint between the graphite nosetip and the beryllium heat shield. Equilibrium chemistry was included in the computations.[68] Limited details are available for this computations, and Zoby has commented (private communication, August 1996) that the mean heating in the Malik et al. computations appeared high. These results are valuable, but it seems that definitive computations for re-entry F remain to be carried out.

Sherman and Nakamura,[46,69] 44-Degree Cone at Reentry

Four flight tests were carried out with this 22-deg half-angle cone, which was constructed with a beryllium skin and a graphite nosetip.[46,69] The vehicles were instrumented with pressure transducers and thermocouples. The first three tests had angles of attack less than 1 deg, whereas the last had an AOA of less than 2 deg. The wall temperature divided by the recovery temperature was about 0.1 at 120 kft, rising to 0.19 at 100 kft. Transition occurred at altitudes between about 120 and 100 kft, at a local (edge) Mach number of about 6. Transition Reynolds numbers based on arclength were about 4×10^6 at transition onset, and varied from about 4×10^6 to about 12×10^6 at the end of transition (depending on position along the vehicle). Transition Reynolds numbers based on momentum thickness were 600–900 at transition onset, and 800–1300 at the end of transition. Because the details of the geometry and trajectory remain classified, a detailed reanalysis is not yet possible. The relatively low transition Reynolds numbers may possibly be explained by the dramatic destabilizing effect of wall cooling on the dominant second-mode instability at this moderate edge Mach number, although the e^N computations supporting this argument are not well documented.[14]

Mach 22 Cone

Reference 70 describes transition measurements on two flights of 8-deg half-angle beryllium cones during re-entry, one of which occurred at near zero angle of attack. The trajectories in altitude and velocity remain classified (Ref. 70, p. 53) so that detailed computations cannot be performed in comparison. Reference 71 analyzes the transition measurements on flight 2, which re-entered at angles of attack up to 75 deg, but conditions are not reported in enough detail to permit a modern reanalysis.

Space Shuttle Orbiter

Transition onset on the NASA Space Shuttle occurs during re-entry at Mach numbers ranging from 16 to 6 and at length Reynolds numbers ranging from 10×10^6 to 3×10^6 (Ref. 72). The primary cause for the variation is thought to be surface roughness. The three-dimensional distribution of transition in flight is shown in Ref. 73, along with some detail on the freestream conditions. Flight and ground-test data for roughness effects on transition are compared in Ref. 74. At transition in flight, the wall temperature is about one-quarter of the edge temperature, the edge Mach number is about 2–3, and $Re_\theta \simeq 200$–1000. Although the Shuttle is a hypersonic vehicle, the large angle of attack causes a low edge Mach number, so that transition occurs under low supersonic conditions, except insofar as the nose is concerned. Transition extent is a very significant factor

in flight (it is normally given in seconds from re-entry), but data for the Reynolds-number extent have not yet been reduced, to the author's knowledge.

Lower Enthalpy Hypersonic Flight Tests

This section will survey results with peak Mach numbers above 5, regardless of edge Mach number. Although the tests might instead be classified by edge Mach number or the dominance of second-mode instability, such a classification in many cases would require further analysis. Only those papers with explicit transition data will be discussed. There are a large number of other papers in the NACA report database that report only raw heating data, along with model and trajectory details. These might be reanalyzed to determine if useful transition data can be obtained from them, but no attempt was made to survey these publications.

Rabb and Disher,[36] 20-Degree Cone-Cylinder to Mach 5.0

A cone with an included angle of 20 deg was flown to Mach 5.02 (Ref. 36). The cylinder had a 9.25 in. diameter. The tip was sharp, as is evident from the photograph in Ref. 36, but the small bluntness does not seem to have been measured. The surface of the $\frac{1}{32}$-in. Inconel skin was polished to a mirror finish of 1.5–2 μin. Seven platinum resistance-wire temperature-sensing devices were installed on the inside surface of the cone. Heat transfer rates are inferred from the temperature data and are used to confirm transition locations that are first determined from slope changes in the temperature data. The model was launched from an airplane at 36,000 ft and was accelerated under rocket power to lower altitudes during the transition measurements. At each of the seven measurement stations, the flow first transitioned from turbulent to laminar flow and then transitioned back. The maximum transition Reynolds number was 32×10^6 at a local Mach number of 3.56 and a wall to local stream temperature ratio of 1.2. Transition occurred under nearly identical conditions at two stations on opposite sides of the cone, suggesting that the angle of attack was near zero and the polish was nearly uniform. Transition Reynolds numbers ranged from 9 to 20×10^6 during the laminarization and from 17 to 32×10^6 during the retransitioning. A detailed reanalysis needs to be performed to understand the laminarization and retransition. The main limitation appears to be the presence of only 7–10 measurement times during the roughly 1 s of laminar flow. Transition moved forward on the cone during the retransitioning process, but the temporal resolution is very limited. The symmetry of the transition measurements suggests that the angle of attack was near zero. The results appear to warrant further analysis.

Rumsey and Lee,[40,75] 10-Degree Cone to Mach 5.9

A 5-deg half-angle cone was tested at Mach numbers to 5.9 (Refs. 40 and 75). The cone was 40 in. long and was positioned at the nose of a rocket-propelled missile launched from an airplane. Six thermocouples were carefully embedded in the 0.030-in.-thick Inconel skin, all along a single ray. Transition is inferred from heat transfer distributions computed using a heat balance. Stanton numbers are computed using simple sharp-cone theory and are compared to theoretical values obtained from the laminar supersonic cone rule. Conduction within the skin was estimated and then neglected. Roughness as measured by a profilometer was 3–4 μin. on the forward 20 in. and 5 μin. aft. The tip bluntness is apparently small, judging from the photographs, but is not reported. The test of Ref. 38 was carried out with a tip radius of $\frac{1}{16}$ in., and that reference states that the tip in this test was sharp, so that the bluntness must have been much less than $\frac{1}{16}$ in. radius. References 76 and 77 are cited for model details, but contain few additional details; Ref. 77 cites a 0.050-in.-diam pitot hole specially inserted in the nose of one model, implying that the tip bluntness was normally far less than this. The wall-to-static temperature ratio was about 1.2. As vehicle Mach number increased from 1.6 to 3.4, the transition length Reynolds number increased from 7×10^6 to 19×10^6, based on edge conditions. "At a relatively constant Mach number near 3.7, the transition Reynolds number decreased about 30% as the ratio of wall temperature minus adiabatic temperature to stagnation temperature changed from -0.35 to -0.25." At higher Mach numbers, the skin temperatures along the body were between the computed laminar and turbulent values, possibly indicating a long intermittent region.

The major limitation of this test[40,75] is the lack of AOA data. AOA information must be inferred from the agreement between the measured and computed Stanton number distributions. The theoretical and experimental values differ by as much as a factor of 2. Because the agreement was not significantly better when the authors assumed an AOA of 5 or 10 deg, it appears that it will be difficult to resolve AOA well enough to make further analysis fruitful.

Rabb and Krasnican,[78] 15-Degree Cone–Cylinder to Mach 6.75

A 7.5-deg half-angle cone was tested at Mach numbers to 6.75 (Ref. 78). The model was identical to that used in Ref. 43. The cylindrical afterbody had a diameter of 6 in., and the cone had a hemispherical nosetip with a $\frac{7}{8}$ in. diameter. The thin-skin Inconel model was polished to a 2 μin. finish with a diamond-paste compound. On the inner surface of the skin, 12 thermocouples were installed, 11 along a single ray, with one on the opposite side. The temperatures on opposite sides of the cone agree to within 5%, suggesting that the AOA was small. The temperature data are reduced to heat transfer coefficients for determination of transition location. The static pressure was also measured at one station on the cylinder. The wall-to-stream temperature ratio ranged from 0.3 to 0.8. The temperatures were compared to theoretical values computed based on blunt-tip edge conditions. The far downstream stations appeared to be always turbulent. The analysis of the transition Reynolds number needs to be redone because it was based on sharp-tip conditions, which are probably not valid for this bluntness. The authors state that "Laminar flow was observed on the highly polished cone-cylinder at the maximum sharp-tip Reynolds number of 50.2 million." The maximum blunt-tip laminar Reynolds number is about 9×10^6, according to Ref. 78 computations. The paper was not included in Beckwith's unpublished survey, probably because Beckwith's survey was limited to sharp cones. Two downstream sensors appear to show a transitional temperature rise, but Rabb and Krasnican believed these sensors saw turbulent flow much earlier in the flight because the experimental Stanton numbers were about $\frac{3}{4}$ of the values they computed for turbulent flow from early in the flight.

The data in this report are limited because it is not clear that transition occurred at a measurement station. On the other hand, the symmetrical thermocouple data and the redundant static-pressure and altitude data should allow one to infer angle of attack. The data appear to warrant further investigation.

Rabb and Krasnican,[79] Three 15-Degree Cone–Cylinders to Mach 7.6

Three 7.5-deg half-angle cones were tested at vehicle Mach numbers to 7.6 (Ref. 79). The models had cylindrical afterbodies with diameters of 6 in. The cones had a hemispherical nosetip with a $\frac{7}{8}$ in. diameter. The models were similar to those used in Ref. 78. Surface finishes of 2, 20, and 50 μin. were tested on the three vehicles, which were otherwise nominally identical. Surface roughness was measured both with a profilometer and a surface interferometer, and considerable detail is reported. On the back of the $\frac{1}{16}$-in. Inconel skin, 11 thermocouples were positioned on each of the three thin-skin models. One thermocouple was positioned on the opposite side from the main thermocouple ray, and each model has a single static-pressure port on the cylinder. Transition is inferred from Stanton number coefficients computed using a heat balance and blunt-tip assumptions. The minimum values of wall temperature divided by edge static temperature ranged from $\frac{1}{2}$ to $\frac{1}{3}$, at edge Mach numbers ranging from 2.8 to 3.6. The peak transition Reynolds number based on arclength was 32.9×10^6 when based on sharp-tip assumptions, or 11.5×10^6 when based on blunt-tip assumptions. Transition on the two rougher models "... occurred while the ratios of wall to local stream temperature were decreasing and the local Reynolds numbers were either decreasing or constant." For the cases with 2- and 20-μin. roughnesses, transition occurred at almost exactly the same time on opposite sides of the cone. These data and the redundant static-pressure measurements should allow estimation of AOA effects. The data appear to warrant a detailed analysis with modern techniques.

Garland et al.,[80] Power Law Nose to Mach 6.7

A modified $\frac{1}{10}$-power blunt nose was tested to Mach 6.7 (Ref. 80). The spun-Inconel nose had a base diameter of 6 in., a polish of 6–8 μin. rms, and a thickness of 0.050 in. Measurements were made with six thermocouples mounted along one ray on the inner surface of the skin, and transition was inferred from heating-rate plots. Values of Reynolds number Re_θ at transition onset ranged from 1600 to 350. For freestream Reynolds numbers below 27×10^6/ft, laminar flow was maintained to $Re_\theta \simeq 1000$, as calculated by Garland et al. using approximate methods. During this time, the freestream Mach number increased from 2 to 5. For higher freestream Reynolds numbers and Mach numbers, transition moved suddenly forward. Batt and Legner[49,50] did not analyze this test, because the nose was not hemispherical. The data appear to warrant further analysis. Although AOA is not determined accurately, AOA should have less impact on this blunt-nose test.

Disher and Rabb,[43] 15-Degree Cone–Cylinder to Mach 8.17

The 15-deg included-angle cone had a hemispherical nosetip with a $\frac{7}{16}$ in. radius.[43] The cylinder diameter was 6 in. The cone and cylinder were Inconel, polished to a surface finish of 2 μin. rms. Four thermocouples were installed on the $\frac{1}{16}$-in. Inconel skin, along a single ray. The time dependence of heat transfer is inferred from a heat balance and is used to deduce transition locations. At the peak Mach number, the freestream Reynolds number was 18×10^6/ft, and the flow was laminar to the last measuring station, which was on the cylinder, 29.5 in. from the nose. At this last station, transition occurred at $M_e \simeq 2$ and $Re_s \simeq 11 \times 10^6$, and a wall-to-stream temperature ratio of 1.2, where the conditions are computed assuming the local flow has passed through a normal shock at the blunt tip. If the computations are performed using sharp-tip conditions, the flow remained laminar to $Re_s \simeq 28 \times 10^6$ at $M_e = 3.6$ and a temperature ratio of 1.9. The data are less valuable because of the few thermocouples and the lack of any redundancy that could be used to infer AOA.

Krasnican and Rabb,[42] 15-Degree Cone–Cylinders to Mach 8.50

The three highly polished cone–cylinders had 15-deg included angles and cylinder diameters of 6 in. (Ref. 42). The three had hemispherical tips with diameters of 2, 3, and 4 in. and were finished to an rms roughness of 2 μin. The models were made of 0.060-in.-thick Inconel or nickel, and each contained a pressure tap, 2 accelerometers, and 10 thermocouples. The thermocouples were mounted flush with the outer surface of the skin; nine were along the primary ray, with one on the opposite side. The skin thickness at each thermocouple station is reported. The models were rocket launched from high altitude in a zero-lift trajectory. The model with the 2-in. nose remained laminar throughout the flight, except at the thermocouple on the secondary ray, which appears to transition at 1.2 s. At this time, the freestream Reynolds number was about 7×10^6/ft, the total pressure was about 45 psia, and the cone surface pressure was about 3.7 psia; the local length Reynolds number was about 2×10^6, assuming zero angle of attack, and had decreased from a maximum of about 3.6×10^6. The model with the 3-in. nose yielded transition data at all points aft of the nose. Transition occurred at length Reynolds numbers varying from 0.8 to 5.9×10^6, depending on position. Remarkably, these Reynolds numbers are no larger than those found on the 2-in. nose model, yet the 2-in. nose model remained laminar. The local wall-to-stream temperature ratios range from 0.6 to 0.8 at transition. Transition on the two thermocouples located on opposite sides of the cone occurred at significantly different times.

On the model with the 4-in. nose, most thermocouples began with transitional heat transfer rates, laminarized, retransitioned, and then in some cases laminarized again. Local transition Reynolds numbers varied from 0.6 to 5×10^6, depending on position, at local Mach numbers ranging from 1.05 to 3.01, with wall-to-stream temperature ratios from 0.27 to 1.51. This model had two symmetrically placed thermocouples, which exhibit heat transfer rates and transition times that appear nearly the same.

For all three models, the cone static pressure can be ratioed to the total pressure and compared against theory to check the AOA. Figure 16 in Ref. 42 shows such a computation, based on an approximate method. The Ref. 42 figure suggests that the models were at nearly zero AOA for about half of the accelerating period. The model with the 4-in. nose seems to have the smallest AOA, and it also has the most symmetrical transition locations. A reanalysis of the data appears to be warranted. Such a reanalysis might well provide important information regarding bluntness effects.

Bond and Rumsey,[81] 25-Degree Cone–Cylinder–Flare to Mach 9.89

A blunted cone with a 12.5-deg half-angle and an 8.5-in.-diam cylindrical afterbody was flown to Mach 9.89 (Ref. 81). The aft flare had a compression angle of 10 deg. The nose bluntness was 0.60 in. diam with a primary radius of 1 in.; a drawing of the shape is given in Ref. 81. Profilometer measurements of the roughness yielded 10–12 μin. on the (preoxidized) nose surface and 2–3 μin. on the forward portion of the nose. Oxidizing increased the nose roughness from 3.5–7 μin. to 10–12 μin. The model was 6.68 ft long. Five pressure sensors were installed: one on the cone, one on the cylinder, and three on the flare. The pressure data appear to be sufficient to infer the AOA. The Inconel skin was 0.032 in. thick and had 24 thermocouples spot welded to the inside. The skin thickness at the thermocouple stations is tabulated. Five thermocouples were installed along a secondary ray, on the opposite side of the main ray. The thermocouple temperatures are given, and the data were reduced to heat transfer coefficients, using a heat balance, in Ref. 82. The freestream Reynolds numbers ranged up to 1.21×10^6/ft. Above about Mach 4.5, analyses based on the thermocouple and pressure data suggest that the model was not at zero AOA. On some sensors the flow transitioned, relaminarized, and transitioned again. Transition Reynolds numbers varied from $Re_s \simeq 3$ to 15×10^6, at local Mach numbers from 1.5 to 3.5, and wall-to-stream temperature ratios of 1–2. Although the pressure data show damped fluctuations after the fourth-stage rocket firing, the last 3 s of telemetry show fairly stable conditions, during which the freestream Mach number is about 9. For these hypersonic conditions, it appears possible to infer AOA and possibly roll angle from the pressure and surface temperature data, using modern analysis methods.

Supersonic Flight Tests

Buglia,[83] Hemispherical Nose at Mach 3

A highly polished hemisphere cone with a 13-in.-diam Inconel nose was flown at zero AOA to Mach 3.14 (Ref. 83). The nose section of the 0.032-in. Inconel skin was polished to 2–3 μin. rms, whereas the conical section was polished to 3–5 μin. rms. Measurements were made with 12 thermocouples spot welded to the inside of the skin along a single ray. Transition was determined from Stanton number distributions computed using a thin-wall heat balance. Six static pressure measurements were also made, along a second ray. The laminar boundary layer was computed using the modified Newtonian pressure distribution and the method of Ref. 84. The value of Reynolds number Re_θ at transition ranged from 800 to 2200; it decreased with increasing Mach number and unit Reynolds number, as might be expected for roughness-dominated transition. The wall was cold; $T_w/T_e \simeq 0.5$–1.

Batt and Legner[50] report limited attempts to correlate transition on this model with the surface roughness; they quote $(k/\theta)(T_e/T_w) = 0.03$ for this test. The k calculation of Ref. 50 is from measurements made in a polished cross-sectional plane by applying a transformation outlined by Dirling.[85] Definition of surface roughness is a complex issue; according to Reda (private communication, October 1997), Batt and Legner,[50] incorrectly applied the Dirling transformation. The Dirling transformation can be used to convert an average measured in-plane roughness height to an average three-dimensional roughness element height by applying a geometrical scale factor, which is $4/\pi$ for hemispherical shapes or 2 for conical shapes. However, these simple scaling factors cannot be applied to any other in-plane roughness heights, such as the 30-percentile exceedance value, as was done in Refs. 49 and 50.

The roughness Reynolds number was computed by Merkle (Ref. 86, p. 29) as $Re_k = 0.7$, where Re_k is based on conditions in the smooth-wall boundary layer at the roughness height k. This result should be checked, however, because Merkle's p. 100 quotes the roughness height as 0.0002 in. (an estimate of the peak roughness?),

whereas he quotes the roughness as 20 microns on p. 29 in Sec. 3.2.8. (Ref. 86). This Reynolds number Re_k is much smaller than the value of about 10 used for specifying the polish in the throats of quiet wind-tunnel nozzles.[87] If correct, it is thus much smaller than any that has ever been suggested as likely to cause transition. Buglia's work embodies the blunt-body paradox[59,60] because the transition on the nose is not readily explained either by roughness or by instability.[86] Further reanalysis of the data appears warranted.

Garland and Chauvin,[88] Hemisphere–Cylinder at Mach 3.88

A polished hemisphere–cylinder of 8 in. diameter was flown to a Mach number of 3.88 (Ref. 88). The Inconel nose was polished to 25-μin. rms as measured with a profilometer, whereas the magnesium cylinder was polished to about 60-μin. rms. Thermocouples were installed on the inner surface of the skin at 23 locations along one ray; the skin thickness at the thermocouple stations is reported. A heat balance is used to infer Stanton number distributions, from which transition is inferred. The wall was cold; $T_w/T_e \simeq 0.5$–1.0. Reference 88 describes the transition as follows.

> If the Reynolds number to the junction [of the hemisphere–cylinder] is greater than approximately 6 million, transition appeared in the subsonic flow region, and the Reynolds number of transition is low (0.8 to 3 million); however, when the Reynolds number [to the junction, Re_s] was less than 6 million, transition occurred in the supersonic region, and the Reynolds number of transition may vary from 7 to 24.7 million.

On the cylinder, the transition-onset Reynolds number Re_θ was as high as 1900 at a freestream Mach number of 3.4. Transition did not move aft of a joint placed 28.25 in. downstream of the nose, presumably due to roughness. When transition occurred on the hemisphere, Reynolds number Re_θ was about 300. Batt and Legner[50] report $(k/\theta)(T_e/T_w) = 0.3$–0.5 for this test, which had a roughness about 10 times that in Buglia's test.[83] The considerably lower transition Reynolds numbers observed on the nose are attributed to this higher roughness. The transition on the cylinder has never been analyzed in detail; Re_θ/M_e must be very large for this transition data. Although there are no data from which to infer AOA, it may not be critical for this blunt body. The computations were carried out using older methods, and the data appear to warrant a reanalysis.

Hall et al.,[89] Hemisphere–Cylinder at Mach 3

Another polished hemisphere–cylinder of 8 in. diameter was flown,[89] to a Mach number of 3, to repeat Buglia's measurements.[83] The spun-Inconel nose was polished to a 1–5 μin. finish, as measured with an interference microscope. The cylinder section was polished to 3–8 μin. rms, and "imperfections of undetermined depth existed at the hemisphere–cylinder junction." Measurements were made along rays 180 deg apart using 20 thermocouples. The thermocouples were welded to the inside of the 0.032-in. skin; the skin thickness at each thermocouple is reported. Stanton number distributions were computed from a heat balance and used to infer transition location.

In the earlier, powered part of the flight, transition occurred on the nose at $Re_\theta = 900$–1400, freestream Mach numbers of 2–3, and freestream unit Reynolds numbers of 14–17 $\times 10^6$/ft. In the later, unpowered part of the flight, transition moved downstream to the cylinder section. A flaw was noted on one side of the cylinder–hemisphere junction, during polishing. This appears to be connected to a large difference in the transition Reynolds numbers for the thermocouple arrays on the two sides of the cylinder. Transition-onset Reynolds number Re_θ for the bottom ray ranged from 1470 to 1260 during this time, whereas on the upper side the value ranged from 3680 to 3340. Accelerometer data are used to infer that this difference could not have been caused by AOA, which is stated to be within 0.4 deg of zero during this period of the flight. The ranges for Reynolds number Re_s are 3–4 $\times 10^6$ and 10–15 $\times 10^6$ for the two rays. The wall was cold, because T_w/T_e ranged from 0.5 to 1, and T_w/T_e is plotted along with the local edge Reynolds number and Stanton number distributions. Transition extent can be inferred from the Stanton distributions, and ranges from roughly 100% to 20% of the distance to transition onset. The results were compared those of Garland and Chauvin,[88] who had a 25-μin. roughness (see earlier description). The high polish on the nose appears to be the critical factor, allowing achievement of a much higher transition Reynolds number for transition on the nose. The high values are also in rough agreement with Buglia.[83] The data are discussed by Batt and Lagner,[50] but are not analyzed in detail in Ref. 50 because transition occurred for $M_e > 1$. The data appear to warrant reanalysis with modern methods.

Chauvin and Speegle,[44] Blunt and Sharp Cones to Mach 4.7

The two cones of Ref. 44 had included angles of 50 deg and base diameters of 17.7 in. One was sharp, with a 0.078-in. tip radius, and the other was blunt, with a 4.44-in. tip radius. Both models were finished to an rms roughness of 25 μin. measured with a profilometer, prior to oxidizing the Inconel to stabilize the emissivity. No roughness measurements were made after oxidation. The blunt nose contained 12 thermocouples and 6 pressure taps, whereas the sharp nose had only the 12 thermocouples. The thermocouples were installed along a single ray, on the inner surface of the 0.031-in.-thick skin. Stanton numbers were computed using a heat balance and were used to infer transition location. The models were rocket launched from the ground. On the blunt model, transition occurred on the nose at a length Reynolds number between 1 and 2 $\times 10^6$. At transition, $Re_\theta \simeq 320$–380 at freestream Mach numbers of 2.5–4.7, at a location 22 deg from the nose. The pressure measurements suggest that the AOA was small. On the sharp model, transition also occurred at $Re_s \simeq 1$–2 $\times 10^6$. The wall-to-freestream temperature ratio was about 1. The authors believe that the transition occurred much earlier than in Ref. 83 because of the higher surface roughness. The large half-angle of the cone may also be a factor, at least for the sharp cone.[90] Reanalysis appears warranted.

Sternberg,[91,92] 20-Degree Cone to Mach 3 on a V-2

A 8-ft long, 10-deg half-angle cone was flight tested at Mach 3 using a V-2 rocket.[91,92] The AOA was held to within 1 deg of 0.0, the wall was cold, and the nose radius was small but is not given. Reynolds number Re_s at transition was clearly documented to reach 40 $\times 10^6$ at station 43 N (apparently based on local edge conditions, which are nearly the same as freestream if the bluntness is small). Some data for a transition $Re_s = 90 \times 10^6$ are presented. These are both apparently transition-onset values, but the results are not well documented. The results are of historical value because at the time they seemed to validate early theories on the complete stabilization of supersonic boundary layers using sufficient wall cooling.

Merlet and Rumsey,[38] 10-Degree Cone–Cylinder to Mach 3.5

The cone had a 10-deg included angle and a tip diameter of $\frac{1}{8}$ in. (Ref. 38). The 0.080-in.-thick skin was made of copper to achieve low surface temperatures. The cone was 100 in. long, with a weld joint at 58.5 in. The tip was steel. Profilometer measurements of the surface roughness yielded values of 10–16 μin. rms, although optical measurements of the same yielded values that were 8–10 times larger. Along a single ray, 12 thermocouples were installed in the skin of the model. Heat transfer rates are inferred from a standard thin-skin heat balance and are tabulated. Transition locations are inferred from the distribution of Stanton numbers. The model was launched by rocket from the ground. The flow was initially turbulent, then laminarized at the upstream station after acceleration ends. Laminar flow moved aft as the model decelerated. Stanton numbers are intermediate between the computed laminar and turbulent values over large regions of the vehicle at some times. Transition Reynolds numbers vary from $Re_s \simeq 6$ to 33 $\times 10^6$, at local Mach numbers from 2 to 3.3, and local ratios of wall-to-stream temperature of 1.5–1.9. These values are probably computed using sharp-tip theory. Laminar flow only occurs on the first 30 in. of the model. The authors,[38] speculate that the transition Reynolds numbers are larger than in Ref. 40 because of the tip bluntness, although the surface is rougher. The entropy-layer swallowing length should be computed for this model to categorize the probable bluntness effect. However, because there are no redundant data from which to infer AOA, further analysis may not be warranted.

Rumsey and Lee,[39] 15-Degree Cone–Cylinder–Flare to Mach 4.7

The cone had an included angle of 15 deg, with a 10-deg half-angle flare (Ref. 39). The 0.03-in.-thick Inconel skin had 23 thermocouples spot welded to its inner surface, along a single ray: 12 on the cone, 5 on the cylinder, and 6 on the flare. The skin thicknesses at the thermocouple stations are tabulated, along with the raw temperature and Reynolds number data. Heat transfer rates were inferred from the thin-skin heat balance and were used to deduce transition locations. The nose diameter was about 0.02 in.; the cylinder diameter was 8.5 in. The usual profilometer measurements gave rms roughnesses on the preoxidized surfaces of 8–15 μin. for the nose cone and 6–10 μin. for the cylinder and flare. Optical measurements of the same surface roughnesses were 3–4 times larger. AOA was estimated from transverse accelerations and was less than 1 deg up to third-stage separation at Mach 4.7, after which it increased to 8 deg over 3 s. The azimuthal angle of the thermocouple plane is given during this period. Transition Reynolds numbers ranged from $Re_s \simeq 4$ to 19×10^6, increasing as the Mach and Reynolds numbers increased. The wall-to-stream temperature ratio was about 2 at transition, with local Mach numbers ranging from 3 to 5. The peak values are lower than in Ref. 41, and the authors[39] believed this was due to the increased roughness associated with the preoxidation of the nose. Table 2 and Fig. 1 here show these data lying at relatively low transition Reynolds numbers. The data are tabulated, and appear to warrant a reanalysis.

Rabb and Simpkinson,[37] 20-Degree Cone–Cylinder to Mach 4.9

Two 20-deg included-angle cone–cylinders were air launched at 36,000 ft and accelerated to Mach 4.9 by rockets, along zero-lift trajectories.[37] The cylinders had diameters of 9.25 in. The cone was separated into two sections by ceramic rings, which imposed a surface discontinuity of about 0.003 in. The models were polished to a mirror finish, which is evident in the photograph[37] but is not documented. The tip appears sharp but is not documented. Each cone had seven platinum temperature sensors, attached to the inner surface of the 0.03-in.-thick Inconel skin. Each also included a linear accelerometer, a static-pressure orifice, and a total-pressure probe. Model 3 was at lower altitude when at comparable flight speeds, due to a delay in rocket ignition, and the flow on it was completely turbulent. Stanton number plots show that heat transfer increases by a factor of 3–4 at transition, at the five operational thermosensors on model 4. One of the five thermosensors is opposite the main ray. Stanton numbers were computed from a thin-skin heat balance and were used to deduce transition locations. All of the thermosensors were downstream of the ceramic ring. Transition occurred under nearly identical conditions on two sensors on opposite sides of the model, indicating the flow was nearly symmetric. The local transition Reynolds number Re_s was about 8×10^6 at all stations, at freestream Mach numbers ranging from 1.8 to 2.5. At transition, the local skin temperature was about equal to the local stream temperature. Because the pressure data and the symmetrical thermosensor data suggest that it is possible to infer AOA, the data appear worthy of further analysis, despite the limited information about nose sharpness and surface roughness.

Rumsey and Lee,[41] 15-Degree Cone–Cylinder–Flare to Mach 5.2

The cone had a 15-deg included angle and a nose radius of about 0.010 in. (Ref. 41). The cylinder diameter was 8.5 in., and the cone was polished to an rms roughness of 6–10 μin. as measured with a profilometer. The two-stage rocket was launched from the ground. The nine thermocouples were spot welded to the inside surface of the 0.027-in.-thick Inconel skin, along a single ray. Heat transfer rates are inferred from a thin-skin heat balance and are used to deduce transition location. The results generally show transition to turbulence and then a relaminarization. The transition-onset length Reynolds number Re_s varies from 14 to 30×10^6, at vehicle Mach numbers varying from 1.4 to 4.6. The wall-to-stream temperature ratios vary from 1.2 to 2.5. The extent of the transitional region varies in length Reynolds number from 5 to 18×10^6. From $t = 17.25$ to $t = 17.75$ s, transition onset moves from 11 in. to 12.5 in., while the end of transition moves from about 20 in. to about 15 in., while the freestream conditions change little. There is no data on the AOA, which was nominally zero. Heat transfer increases by a factor of 5 at transition. Because there are no redundant data to aid in inferring AOA, further analysis may not be warranted.

X-15 Wing, Ball Nose, and Vertical Fin

Considerable heating data were obtained on the X-15 airplane, but most of the flow was turbulent due to some fairly large roughnesses (see Ref. 93 for an overall review). Primary data were obtained with 293 surface thermocouples, along with 136 surface-pressure orifices.[94] Reference 94 shows paint images and heating patterns caused by transition on the wing, which was tripped by surface discontinuities created by 0.015–0.027 in. expansion joints at the leading edge.[93] When shields were placed over joints, transition was thought to be delayed somewhat, but quantitative results are not presented. Reference 93 reports that the covers actually had larger roughness than the original joints and that buckling occurred at the joints in flight due to thermal expansion and implies that transition was not delayed by installation of the covers. Some additional wing transition data are presented in Fig. 10b of Ref. 95, where transition appears to have occurred between 4 and 10% chord, during a high-altitute re-entry flight. The freestream conditions are changing rapidly during the flight, so that a full coupled boundary-layer/skin-heating computation would be necessary to determine transition location.

Transition may also have occurred on the ball nose (Ref. 94, p. 9) because the heating rate on the thermocouple at 80 deg was in some cases well above the laminar calculations, although the heating rate at the 20-deg thermocouple was in good agreement with the calculations. There were originally three thermocouples on the nose, at 20, 50, and 80 deg, all in a row on the horizontal reference plane. A pressure orifice was located between the 20- and 50-deg thermocouple; the roughness from this orifice may be significant. The thermocouples were located on the inside surface of the ball nose, and so they should not have created any roughness. Reference 95 tabulates details of a high-altitude flight in which transition must have occurred, and Refs. 96 and 97 have further details on the geometry.

A 0.172-in. forward-facing step existed between the ball nose and the fuselage.[93] This step appears to have tripped transition on the lower fuselage under most conditions (Ref. 94, p. 9). Reference 95 tabulates details of the flight conditions and thermocouple readings for a high-altitude flight, which appears to contain a record of this transition tripping.

Reference 98 contains additional data for transition on the vertical fin of the X-15. Transition was determined from sound pressure measurements using surface-mounted microphones. The transition Reynolds numbers on the fin are relatively low, in the range of conventional-tunnel flat plate data, with $Re_s \simeq 3 \times 10^6$, at Mach numbers of about 3. This is probably because the fin is subject to sound radiation from the turbulent boundary layer on the fuselage and also because it was fairly rough.

Because transition on the X-15 was apparently dominated by roughness, reanalysis of the data may aid in determining allowable roughness criteria. In the cases just described, it appears that the conditions are documented well enough to permit such a reanalysis.

Banner et al.,[99] Swept Wing at Mach 2

Transition measurements were obtained on a fighter-plane wing at Mach numbers up to 2.0 and at a sweep angle of 26.9 deg (Ref. 99). Photographs[99] of sublimating chemicals were taken in flight to observe transition location. Surface roughnesses of 25, 13, and 7 μin. were compared, as were surface wavinesses of 0.006 and 0.012 in./in. Streamwise streaks were observed, suggesting transition caused by stationary crossflow vortices. The length Reynolds numbers for transition, Re_s, varied from 2 to 8×10^6, depending on conditions.

Fisher and Dougherty[55] and Dougherty and Fisher,[56] Cone in Flight to Mach 2

Fisher and Dougherty[55] and Dougherty and Fisher[56] obtained measurements on a sharp 5-deg half-angle cone in flight, as well as in various wind tunnels. Freestream Mach numbers ranged from 0.5 to

2.0. Measurements were made with a high-frequency traversing pitot tube, as well as with microphones in the cone surface. Freestream noise is a critical issue for wind-tunnel measurements (see Ref. 25), and the flight values of freestream noise data that were obtained with the pitot tube form a unique benchmark. Transition Reynolds numbers were as high as $Re_s \simeq 1 \times 10^7$ at the higher Mach numbers.

Hollow Cylinder at Mach 2.9 Below an SR-71

Heating measurements were obtained on a 3.04-m-long hollow cylinder suspended below the SR-71 airplane in flight at Mach 2.9 (Ref. 100). The wall-to-recovery temperature ranged from 0.66 to 0.91, and the local unit Reynolds number was about 4.3×10^6/m. The cylinder had a 0.437 m diameter and a leading-edge radius of 0.127 mm. The AOA was less than 0.1 deg. Measurements were made with a pitot rake, a skin-friction gauge, thermocouples, and pressure sensors. The primary measurements were made on the lower surface, away from the fuselage. Flight 3 was carried out at cold-wall temperatures, with a wall temperature of about 350 K. Flights 1 and 2 were carried out at temperatures near radiation equilibrium, at 550 K. Transition onset in flight 2 was measured at $x = 0.76$ m and $Re_s = 3.4 \times 10^6$, with transition end at $x = 1.22$ m and $Re_s = 5.5 \times 10^6$. These values seem low, presumably because of noise radiated from the fuselage of the SR-71 because the cylinder was located within the shock generated by the fuselage (Quinn, private communication, August 1996). This noise can couple into the lower-surface boundary layer at the leading edge. Flight 1 was very similar to flight 2. In flight 3, at cold-wall conditions, transition happened very near the nose, which was unexpected because wall cooling is normally expected to be stabilizing. The surface roughness may have caused the early transition because a cold wall normally has a thinner boundary layer in which roughness is more critical. Although the roughness was not reported, Quinn stated that the stainless steel was polished, although not with diamond compound or to a mirror finish. The test remains interesting because of the limited and relatively well-defined sound radiation from the fuselage.

Discussion and Summary

More than 20 flight tests of high-speed transition have been surveyed. Modern computational comparisons are also described, although these are few in number and often incomplete. A large amount of high-speed data exists in a fairly well-documented form. Reshotko from Case Western Reserve University worked at NACA Lewis Research Center during the 1950s. He worked with the transition flight-test group on occasion and has commented (private communication, 1997) that 1) he believes the work of this group (Disher, Rabb, Krasnican, and others) is of good quality, and 2) the data are worthy of reanalysis with modern techniques. Beckwith and Stainback (private communication, 1997) from NASA Langley Research Center likewise were somewhat familiar with the work of the NACA Langley Research Center flight-test group (Rumsey and Lee and others) and they also believe that the data should generally be of good quality.

The high cost of flight tests means that it will not be possible to repeat much of this work in the near future. Nor can additional flight tests be justified until the features and problems with the current database are clearly identified. Much of the existing database appears to be documented well enough to allow detailed computational comparisons to be performed. Original paper copies of the reports are still available, with original photographs of the models. The basic vehicle data appear to be recorded in sufficient detail, in most cases. It appears that the major limitation will be the problem of determining AOA because the documentation of AOA in flight is limited in most of the NACA work. It may be that redundant thermocouple measurements and ancillary pressure measurements can be used to infer the flight AOA for at least some of the tests. It is hoped that this survey paper will 1) allow designers to readily access flight data that is as close to their design conditions as the database allows and 2) stimulate additional work comparing the database to modern computations.

Acknowledgments

The author's research is funded by the Air Force Office for Scientific Research (AFOSR) Grant F49620-97-1-0037, once monitored by L. Sakell and now monitored by S. Walker. P. C. Stainback and I. E. Beckwith, both retired from NASA Langley Research Center, were of great assistance, through collecting and sorting the work done by them in the 1970s but incompletely published. Dennis Bushnell from NASA Langley Research Center and Eli Reshotko from Case Western Reserve University both encouraged the effort, and both have supplied many obscure references over the past 7 years. Richard Batt from TRW supplied his entire collection of open-literature blunt-nose transition papers. Kenneth Stetson from the U.S. Air Force Research Laboratory provided helpful comments and suggestions. The following are gratefully acknowledged for their private communications: D. Kuntz and W. E. Williamson (1997), K. W. Iliff and W. E. Williamson (September 1996), E. V. Zoby (August 1996), D. Reda (October 1997), and R. D. Quinn (August 1996).

References

[1]Reshotko, E., "Boundary Layer Instability, Transition, and Control," AIAA Paper 94-0001, Jan. 1994.

[2]Hingst, U. G., "Laminar/Turbulent Flow Transition Effects on High Speed Missile Domes," *Missile Aerodynamics*, AGARD CP-493, 1990, pp. 27-1–27-8.

[3]Korejwo, H. A., and Holden, M. S., "Ground Test Facilities for Aerothermal and Aero-Optical Evaluation of Hypersonic Interceptors," AIAA Paper 92-1074, Feb. 1992.

[4]*Sustained Hypersonic Flight*, AGARD CP-600, Vol. 3, April 1997.

[5]Lin, T. C., Grabowsky, W. R., and Yelmgren, K. E., "The Search for Optimum Configurations for Re-Entry Vehicles," *Journal of Spacecraft and Rockets*, Vol. 21, No. 2, 1984, pp. 142–149.

[6]Holden, M. S., "Aerothermal Characteristics of Shock/Shock Interaction Regions in Hypersonic Flows," *Sustained Hypersonic Flight*, AGARD CP-600, Vol. 3, April 1997, Paper C12.

[7]Bushnell, D. M., "Notes on Initial Disturbance Fields for the Transition Problem," *Instability and Transition*, edited by M. Y. Hussaini and R. G. Voigt, Vol. 1, Springer–Verlag, Berlin, 1990, pp. 217–232.

[8]Floryan, J. M., "On the Görtler Instability of Boundary Layers," *Progress in Aerospace Science*, Vol. 28, 1991, pp. 235–271.

[9]Saric, W. S., "Görtler Vortices," *Annual Review of Fluid Mechanics*, Vol. 26, 1994, pp. 379–409.

[10]Mack, L. M., "Boundary Layer Linear Stability Theory," *Special Course on Stability and Transition of Laminar Flow*, AGARD Rept. 709, March 1984, pp. 1–81.

[11]Reed, H. L., and Saric, W. S., "Stability of Three-Dimensional Boundary Layers," *Annual Review of Fluid Mechanics*, Vol. 21, 1989, pp. 235–284.

[12]Herbert, T., "Secondary Instability of Boundary Layers," *Annual Review of Fluid Mechanics*, Vol. 20, 1988, pp. 487–526.

[13]Narasimha, R., "The Laminar–Turbulent Transition Zone in the Turbulent Boundary Layer," *Progress in Aerospace Science*, Vol. 22, 1985, pp. 29–80.

[14]Malik, M. R., "Prediction and Control of Transition in Supersonic and Hypersonic Boundary Layers," *AIAA Journal*, Vol. 27, No. 11, 1989, pp. 1487–1493.

[15]Kufner, E., Dallman, U., and Stilla, J., "Instability of Hypersonic Flow Past Blunt Cones—Effects of Mean Flow Variations," AIAA Paper 93-2983, July 1993.

[16]Schrauf, G., Perraud, J., Vitiello, D., and Lam, F., "A Comparison of Linear Stability Theories Using F100-Flight Tests," AIAA Paper 97-2311, June 1997.

[17]Kleiser, L., and Zang, T., "Numerical Simulation of Transition in Wall-Bounded Shear Flows," *Annual Review of Fluid Mechanics*, Vol. 23, 1991, pp. 495–537.

[18]Herbert, T., "Boundary-Layer Transition—Analysis and Prediction Revisited," AIAA Paper 91-0737, Jan. 1991.

[19]Herbert, T., "Parabolized Stability Equations," *Special Course on Progress in Transition Modelling*, AGARD Rept. 793, 1994, pp. 4/1–4/34.

[20]Herbert, T., "On the Stability of 3D Boundary Layers," AIAA Paper 97-1961, June 1997.

[21]Hu, S. H., and Zhong, X., "Hypersonic Boundary-Layer Stability over Blunt Leading Edges with Bow-Shock Effects," AIAA Paper 98-0433, Jan. 1998.

[22]Chang, C.-L., Vinh, H., and Malik, M. R., "Hypersonic Boundary-Layer Stability with Chemical Reactions Using PSE," AIAA Paper 97-2012, June 1997.

[23]Hudson, M. L., Chokani, N., and Candler, G. V., "Linear Stability of Hypersonic Flow in Thermochemical Equilibrium," *AIAA Journal*, Vol. 35 No. 6, 1997, pp. 958–964.

[24]Beckwith, I. E., and Miller, C. G., III, "Aerothermodynamics and Transition in High-Speed Wind Tunnels at NASA Langley," *Annual Review of Fluid Mechanics*, Vol. 22, 1990, pp. 419–439.

[25]Reed, H., Kimmel, R., Arnal, D., and Schneider, S., "Drag Prediction

and Transition in Hypersonic Flow," *Sustained Hypersonic Flight*, AGARD CP-600, Vol. 3, April 1997, Paper C15; also AIAA Paper 97-1818, June 1997.

[26]Pate, S. R., and Schueler, C. J., "Radiated Aerodynamic Noise Effects on Boundary-Layer Transition in Supersonic and Hypersonic Wind Tunnels," *AIAA Journal*, Vol. 7, No. 3, 1969, pp. 450–457.

[27]Pate, S. R., "Dominance of Radiated Aerodynamic Noise on Boundary-Layer Transition in Supersonic/Hypersonic Wind Tunnels," Arnold Engineering Development Center, AEDC-TR-77-107, Arnold AFB, TN, March 1978.

[28]Schneider, S. P., "Survey of Flight Data for Boundary-Layer Transition at Hypersonic and Supersonic Speeds," AIAA Paper 98-0432, Jan. 1998.

[29]Malik, M. R., Spall, R. E., and Chang, C.-L., "Effect of Nose Bluntness on Boundary Layer Stability and Transition," AIAA Paper 90-0112, Jan. 1990.

[30]Potter, J. L., "Boundary-Layer Transition on Supersonic Cones in an Aeroballistic Range," *AIAA Journal*, Vol. 13, No. 3, 1975, pp. 270–277.

[31]Reda, D. C., "Boundary-Layer Transition Experiments on Sharp, Slender Cones in Supersonic Free Flight," *AIAA Journal*, Vol. 17, No. 8, 1979, pp. 803–810.

[32]Beckwith, I. E., "Development of a High Reynolds Number Quiet Tunnel for Transition Research," *AIAA Journal*, Vol. 13, No. 3, 1975, pp. 300–306.

[33]Stetson, K. F., "Hypersonic Boundary-Layer Transition," *Advances in Hypersonics: Defining the Hypersonic Environment*, Birkhauser, Boston, 1992, pp. 324–417.

[34]Beckwith, I. E., and Bertram, M. H., "A Survey of NASA Langley Studies on High-Speed Transition and the Quiet Tunnel," NASA TM-X-2566 (NASA Database Citation 72N26239), July 1972.

[35]Bertram, M. H., and Beckwith, I. E., "NASA-Langley Boundary Layer Transition Investigations," *Boundary Layer Transition Study Group Meeting, Vol. 3, Session on Ground Test Transition Data and Correlations*, U.S. Air Force Rept. BSD-TR-67-213, Vol. 3, Paper 18, Aug. 1967; also The Aerospace Corp., Rept. TR-0158(S3816-63)-1, Vol. 3, El Segundo, CA (Defense Technical Information Center Citation AD384006; also NASA Database Citation 68X11187).

[36]Rabb, L., and Disher, J. H., "Boundary-Layer Transition at High Reynolds Numbers as Obtained in Flight of a 20-Deg. Cone-Cylinder with Wall to Local Stream Temperature Ratios near 1.0," NACA RM-E55I15 (NASA Database Citation 93R18171), Nov. 1955.

[37]Rabb, L., and Simpkinson, S., "Free-Flight Heat-Transfer Measurements on Two 20-Deg-Cone-Cylinders at Mach Numbers from 1.3 to 4.9," NACA RM-E55F27 (NASA Database Citation 62N63397), July 1955.

[38]Merlet, C. F., and Rumsey, C. B., "Supersonic Free-Flight Measurement of Heat Transfer and Transition on a 10-Deg Cone Having a Low Temperature Ratio," NASA TN-D-951 (NASA Database Citation 62N71525), Aug. 1961; supersedes NACA RM L56L10, 1956.

[39]Rumsey, C. B., and Lee, D. B., "Measurements of Aerodynamic Heat Transfer on a 15-Deg Cone–Cylinder–Flare Configuration in Free Flight at Mach Numbers up to 4.7," NASA TN-D-824 (NASA Database Citation 62N71398), May 1961; supersedes NACA RM L57J10, 1958.

[40]Rumsey, C. B., and Lee, D. B., "Measurements of Aerodynamic Heat Transfer and Boundary-Layer Transition on a 10-Deg Cone in Free Flight at Supersonic Mach Numbers up to 5.9," NASA TN-D-745 (NASA Database Citation 62N71319), May 1961; supersedes NACA RM-L56B07.

[41]Rumsey, C. B., and Lee, D. B., "Measurements of Aerodynamic Heat Transfer and Boundary-Layer Transition on a 15-Deg Cone in Free Flight at Supersonic Mach Numbers up to 5.2," NASA TN-D-888 (NASA Database Citation 62N71462), Aug. 1961; supersedes NACA RM L56F26, 1956.

[42]Krasnican, M. J., and Rabb, L., "Effects of Nose Radius and Extreme Cooling on Boundary-Layer Transition for Three Smooth 15-Deg.-Cone–Cylinders in Free Flight at Mach Numbers to 8.50," NASA MEMO-3-4-59E (NASA Database Citation 63N14756), March 1959.

[43]Disher, J. H., and Rabb, L., "Observation of Laminar Flow on a Blunted 15-Deg. Cone–Cylinder in Free Flight at High Reynolds Number and Free-Stream Mach Numbers to 8.17," NACA RM-E56G23 (NASA Database Citation 62N63995), Oct. 1956.

[44]Chauvin, L. T., and Speegle, K. C., "Boundary-Layer-Transition and Heat-Transfer Measurements from Flight Tests of Blunt and Sharp 50-Deg. Cones at Mach Numbers from 1.7 to 4.7," NACA RM-L57D04 (NASA Database Citation 66N33310), April 1957.

[45]Wright, R. L., and Zoby, E. V., "Flight Boundary Layer Transition Measurements on a Slender Cone at Mach 20," AIAA Paper 77-719, June 1977.

[46]Sherman, M. M., and Nakamura, T., "Flight Test Measurements of Boundary Layer Transition on a Non-Ablating 22-Deg. Cone," AIAA Paper 68-1152, Dec. 1968.

[47]Martellucci, A., Maguire, B. L., and Neff, R. S., "Analysis of Flight Test Transition and Turbulent Heating Data, Part I: Boundary Layer Transition Results," NASA CR-129045 (NASA Database Citation 73N12287), Nov. 1972.

[48]Berkowitz, A. M., Kyriss, C. L., and Martellucci, A., "Boundary Layer Transition Flight Test Observations," AIAA Paper 77-125, Jan. 1977.

[49]Batt, R. G., and Legner, H. H., "A Review of Roughness-Induced Nosetip Transition," AIAA Paper 81-1223, June 1981.

[50]Batt, R. G., and Legner, H. H., "A Review of Roughness-Induced Nosetip Transition," *AIAA Journal*, Vol. 21, No. 1, 1983, pp. 7–22.

[51]Reda, D. C., "Correlation of Nosetip Boundary-Layer Transition Data Measured in Ballistics-Range Experiments," *AIAA Journal*, Vol. 19, No. 3, 1981, pp. 329–339.

[52]Williamson, W. E., "Hypersonic Flight Testing," AIAA Paper 92-3989, June 1992.

[53]Iliff, K. W., and Shafer, M. F., "A Comparison of Hypersonic Flight and Prediction Results," AIAA Paper 93-0311, Jan. 1993.

[54]Malik, M. R., "Instability and Transition in Supersonic Boundary Layers," *Laminar Turbulent Boundary Layers*, Fluids Engineering Div., Vol. 11, American Society of Mechanical Engineers, New York, 1984, pp. 139–147.

[55]Fisher, D. F., and Dougherty, N. S., "In-Flight Transition Measurement on a 10-Deg. Cone at Mach Numbers from 0.5 to 2.0," NASA TP-1971, 1982.

[56]Dougherty, N. S., and Fisher, D. F., "Boundary Layer Transition on a 10-Degree Cone: Wind Tunnel/Flight Data Correlation," AIAA Paper 80-0154, Jan. 1980.

[57]Murphy, J. D., and Rubesin, M. W., "An Evaluation of Free-Flight Test Data for Aerodynamic Heating from Laminar, Turbulent, and Transitional Boundary Layers. Part II—The X-17 Re-Entry Body," NASA CR-70931 (NASA Database Citation 66N20084), April 1965.

[58]Balgeman, E. J., Cassell, G., Dension, M. R., and Tellep, D. M., "X-17 Re-Entry Test Vehicle: R-2 Final Flight Report," Technical Rept. MSD-3003, Lockheed Aircraft Corp. (NASA Database Citation 74N78004), April 1957.

[59]Morkovin, M. V., "Bypass Transition to Turbulence and Research Desiderata," *Transition in Turbines*, NASA CP-2386, May 1984, pp. 161–199.

[60]Stetson, K. F., "Boundary-Layer Transition on Blunt Configurations," NASA Johnson Space Center, Internal Technical Rept. JSC-26528, Feb. 1994.

[61]Murphy, J. D., and Rubesin, M. W., "Re-Evaluation of Heat-Transfer Data Obtained in Flight Tests of Heat-Sink Shielded Re-Entry Vehicles," *Journal of Spacecraft*, Vol. 3, No. 1, 1966, pp. 53–60.

[62]Stainback, P. C., Johnson, C. B., Boney, L. R., and Wicker, K. C., "A Comparison of Theoretical Predictions and Heat-Transfer Measurements for a Flight Experiment at Mach 20 (Reentry F)," NASA TM-X-2560, July 1972.

[63]Johnson, C. B., Stainback, P. C., Wicker, K. C., and Boney, L. R., "Boundary-Layer Edge Conditions and Transition Reynolds Number Data for a Flight Test at Mach 20 (Reentry F)," NASA TM-X-2584, July 1972.

[64]Wright, R. L., and Zoby, E. V., "Flight Measurements of Boundary-Layer Transition on a 5-Deg. Half-Angle Cone at a Freestream Mach Number of 20 (Reentry F)," NASA TM-X-2253, May 1971.

[65]Thompson, R. A., Zoby, E. V., Wurster, K. E., and Gnoffo, P. A., "Aerothermodynamic Study of Slender Conical Vehicles," *Journal of Thermophysics and Heat Transfer*, Vol. 3, No. 4, 1989, pp. 361–367.

[66]Wood, W. A., Riley, C. J., and Cheatwood, F. M., "Reentry-F Flowfield Solutions at 80,000 ft," NASA TM-112856, May 1997.

[67]Malik, M., Zang, T., and Bushnell, D., "Boundary Layer Transition in Hypersonic Flows," AIAA Paper 90-5232, Oct. 1990.

[68]Malik, M. R., "Stability Theory for Chemically Reacting Flows," *Laminar–Turbulent Transition*, Springer–Verlag, New York, 1990, pp. 251–260.

[69]Sherman, M. M., and Nakamura, T., "Flight Test Measurements of Boundary Layer Transition on a Nonablating 22-Deg. Cone," *Journal of Spacecraft and Rockets*, Vol. 7, No. 2, 1970, pp. 137–142.

[70]Haigh, W. W., Lake, B. M., and Ko, D. R. S., "Analysis of Flight Data on Boundary Layer Transition at High Angles of Attack," NASA CR-1913, April 1972.

[71]Johnson, C. B., and Darden, C. M., "Flight Transition Data for Angles of Attack at Mach 22 with Correlations of the Data," NASA TM-X-3235 (NASA Database Citation 75N28377), Aug. 1975.

[72]Bouslog, S. A., An, M. Y., Hartmann, L. N., and Derry, S. M., "Review of Boundary Layer Transition Flight Data on the Space Shuttle Orbiter," AIAA Paper 91-0741, Jan. 1991.

[73]Hartung, L. C., and Throckmorton, D. A., "Computer Graphic Visualization of Orbiter Lower Surface Boundary-Layer Transition," *Journal of Spacecraft and Rockets*, Vol. 24, No. 2, 1987, pp. 109–114.

[74]Bouslog, S. A., Bertin, J. J., Berry, S. A., and Caram, J. M., "Isolated Roughness Induced Boundary-Layer Transition: Shuttle Orbiter Ground Tests and Flight Experience," AIAA Paper 97-0274, Jan. 1997.

[75]Rumsey, C. B., and Lee, D. B., "Measurements of Aerodynamic Heat Transfer and Boundary-Layer Transition on a 10-Deg. Cone in Free Flight at Supersonic Mach Numbers up to 5.9," NACA RM L56B07 (NASA Database Citation 93R18462), April 1956.

[76]Rumsey, C. B., "Free-Flight Measurements of Aerodynamic Heat Transfer to Mach Number 3.9 and of Drag to Mach Number 6.9 of a Fin-Stabilized Cone–Cylinder Configuration," NACA RM-L55G28a (NASA Database Citation 93R18195), Oct. 1955.

[77]Rumsey, C. B., Piland, R. O., and Hopko, R. N., "Aerodynamic-Heating Data Obtained from Free-Flight Tests Between Mach Numbers of 1 and 5," NASA TN-D-216 (NASA Database Citation 78N78522), Jan. 1960; supersedes NACA RM L55A14a.

[78]Rabb, L., and Krasnican, M. J., "Observation of Laminar Flow on an Air-Launched 15-Deg. Cone Cylinder at Local Reynolds Numbers to 50 Million at Peak Mach Number of 6.75," NACA RM-E56L03 (NASA Database Citation 62N64173), March 1957.

[79]Rabb, L., and Krasnican, M. J., "Effects of Surface Roughness and Extreme Cooling on Boundary-Layer Transition for a 15-Deg. Cone–Cylinder in Free Flight at Mach Numbers to 7.6," NACA RM-E57K19 (NASA Database Citation 62N64606), March 1958.

[80]Garland, B. J., Swanson, A. G., and Speegle, K. C., "Aerodynamic Heating and Boundary-Layer Transition on a 1/10-Power Nose Shape in Free Flight at Mach Numbers up to 6.7 and Freestream Reynolds Numbers up to 16 Million," NASA TN-D-1378 (NASA Database Citation 62N13291), June 1962; supersedes NACA RM L57E14a, 1957.

[81]Bond, A. C., and Rumsey, C. B., "Free-Flight Skin Temperature and Pressure Measurements on a Slightly Blunted 25-Deg. Cone–Cylinder–Flare Configuration to a Mach Number of 9.89," NACA RM-L57B18 (NASA Database Citation 93R18905), April 1957.

[82]Lee, D. B., Rumsey, C. B., and Bond, A. C., "Heat Transfer Measured in Free Flight on a Slightly Blunted 25-Deg. Cone–Cylinder–Flare Configuration at Mach Numbers up to 9.89," NACA RM L58G21 (NASA Database Citation 63N20529), Sept. 1958.

[83]Buglia, J. J., "Heat Transfer and Boundary-Layer Transition on a Highly Polished Hemisphere-Cone in Free Flight at Mach Numbers up to 3.14 and Reynolds Numbers up to 24 times 10^6," NASA TN-D-955, Sept. 1961; supersedes NACA RM L57D05.

[84]Lees, L., "Laminar Heat Transfer over Blunt-Nosed Bodies at Hypersonic Flight Speeds," *Jet Propulsion*, April 1956, pp. 259–269.

[85]Dirling, R. B., Jr., "On the Relation Between Material Variability and Surface Roughness," AIAA Paper 77-402, March 1977.

[86]Merkle, C. L., "Stability and Transition in Boundary Layers on Reentry Vehicle Nosetips," U.S. Air Force Office of Scientific Research, AFOSR TR-76-1107 (NASA Database Citation 77N26449), June 1976.

[87]Beckwith, I., Chen, F., Wilkinson, S., Malik, M., and Tuttle, D., "Design and Operational Features of Low-Disturbance Wind Tunnels at NASA Langley for Mach Numbers from 3.5 to 18," AIAA Paper 90-1391, June 1990.

[88]Garland, B. J., and Chauvin, L. T., "Measurements of Heat Transfer and Boundary-Layer Transition on an 8-Inch-Diameter Hemisphere-Cylinder in Free Flight for a Mach Number Range of 2.00 to 3.88," NACA RM-L57D04a, March 1957.

[89]Hall, J. R., Speegle, K. C., and Piland, R. O., "Preliminary Results from a Free-Flight Investigation of Boundary-Layer Transition and Heat Transfer on a Highly Polished 8-Inch-Diameter Hemisphere-Cylinder at Mach Numbers up to 3 and Reynolds Numbers Based on a Length of 1 Foot up to 17.7 Million," NACA RM L57D18c (NASA Database Citation 93R19061), May 1957.

[90]Wilkins, M. E., and Chapman, G. T., "Free Flight Determination of Boundary Layer Transition on Small Scale Cones in the Presence of Surface Ablation," *Proceedings of Boundary Layer Transition Workshop*, Nov. 1971, pp. 3-1–3-21; also The Aerospace Corp., Rept. TOR-0172(S2816-16)-5 (Defense Technical Information Center Citation AD909223).

[91]Sternberg, J., "A Free-Flight Investigation of the Possibility of High Reynolds Number Supersonic Laminar Boundary Layers," *Journal of the Aeronautical Sciences*, Vol. 19, No. 11, 1952, pp. 721–733.

[92]Sternberg, J., "A Free-Flight Investigation of the Possibility of High Reynolds Number Supersonic Laminar Boundary Layers," U.S. Army Ballistic Research Lab., Rept. 821, Aberdeen Proving Ground, MD, June 1952 (Defense Technical Information Center Citation AD-801731).

[93]Braslow, A. L., "Analysis of Boundary-Layer Transition on X-15-2 Research Airplane," NASA TN-D-3487 (NASA Database Citation 66N30177), March 1966.

[94]Banner, R. D., Kuhl, A. E., and Quinn, R. D., "Preliminary Results of Aerodynamic Heating Studies on the X-15 Airplane," NASA TM-X-638, Jan. 1968.

[95]Gord, P. R., "Measured and Calculated Structural Temperature Data from Two X-15 Airplane Flights with Extreme Aerodynamic Heating Conditions," NASA TM-X-1358 (NASA Database Citation 74N71363), March 1967.

[96]Quinn, R. D., and Palitz, M., "Comparison of Measured and Calculated Turbulent Heat Transfer on the X-15 Airplane at Angles of Attack up to 19 Degrees," NASA TM-X-1291 (NASA Database Citation 73N70599), Sept. 1966.

[97]Quinn, R. D., and Olinger, F. V., "Flight-Measured Heat Transfer and Skin Friction at a Mach Number of 5.25 and at Low Wall Temperatures," NASA TM-X-1921 (NASA Database Citation 92N70606), Nov. 1969.

[98]Lewis, T. L., and Banner, R. D., "Boundary-Layer Transition Detection on the X-15 Vertical Fin Using Surface-Pressure-Fluctuation Measurements," NASA TM-X-2466 (NASA Database Citation 72N12994), Dec. 1971.

[99]Banner, R. D., McTigue, J. G., and Petty, G., Jr., "Boundary-Layer-Transition Measurements in Full-Scale Flight," NASA TM-79863 (NASA Database Citation 78N78570), Oct. 1978; rev. NACA RM H58E28, July 1958.

[100]Quinn, R. D., and Gong, L., "In-Flight Measurements on a Hollow Cylinder at a Mach Number of 3.0," NASA TP-1764, Nov. 1980.

T. C. Lin
Associate Editor